JOC Article

A Repertoire of Pyridinium−Phenyl−Methyl Cross-Talk through a Cascade of Intramolecular Electrostatic Interactions

P. Acharya,[†] O. Plashkevych,[†] C. Morita,[‡] S. Yamada,[‡] and J. Chattopadhyaya*,[†]

Department of Bioorganic Chemistry, Box 581, Biomedical Center, Uppsala University, S-751 23 Uppsala, Sweden, and Department of Chemistry, Faculty of Science, Ochanomizu University, Bukyo-ku, Tokyo 112-8610, Japan

jyoti@boc.uu.se

Received October 16, 2002

Direct intramolecular cation−π interaction between phenyl and pyridinium moieties in **1a**$^+$ has been experimentally evidenced through pH-dependent ^{1}H NMR titration. The basicity of the pyridinyl group (pK_a 2.9) in **1a** can be measured both from the pH-dependent chemical shifts of the pyridinyl protons as well as from the protons of the neighboring phenyl and methyl groups as a result of electrostatic interaction between the phenyl and the pyridinium ion in **1a**$^+$ at the ground state. The net result of this nearest neighbor electrostatic interaction is that the pyridinium moiety in **1a** becomes more basic (pK_a 2.92) compared to that in the standard **2a** (pK_a 2.56) as a consequence of edge-to-face cation (pyridinium)−π (phenyl) interaction, giving a free energy of stabilization ($\Delta\Delta G^o_{pKa}$) of −2.1 kJ mol^{-1}. The fact that the pH-dependent downfield shifts of the phenyl and methyl protons give the pK_a of the pyridine moiety of **1a** also suggests that the nearest neighbor cation (pyridinium)−π (phenyl) interaction also steers the CH (methyl)−π (phenyl) interaction in tandem. This means that the whole pyridine−phenyl−methyl system in **1a**$^+$ is electronically coupled at the ground state, cross-modulating the physicochemical property of the next neighbor by using the electrostatics as the engine, and the origin of this electrostatics is a far away point in the molecule—the pyridinyl-nitrogen. The relative chemical shift changes and the pK_a differences show that the cation (pyridinium)−π (phenyl) interaction is indeed more stable ($\Delta\Delta G^o_{pKa}$ = −2.1 kJ mol^{-1}) than that of the CH (methyl)−π (phenyl) interaction ($\Delta\Delta G^o_{pKa}$ = −0.8 kJ mol^{-1}). Since the pK_a of the pyridine moiety in **1a** is also obtained through the pH-dependent shifts of both phenyl and methyl protons, it suggests that the net electrostatic mediated charge transfer from the phenyl to the pyridinium and its effect on the CH (methyl)-π (phenyl) interaction corresponds to ΔG^o_{pKa} of the pyridinium ion (∼17.5 kJ mol^{-1}), which means that the aromatic characters of the phenyl and the pyridinium rings in **1a**$^+$ have been cross-modulated owing to the edge-to-face interaction proportional to this ΔG^o_{pKa} change.

Introduction

Stacking and hydrogen bonding are two most important noncovalent forces that actively contribute to the self-assembly[1,2a,b] of DNA, RNA, and many other nonbiological molecules.[2d−f] While the physicochemical nature of H-bonding is well understood, the nature of ground-state forces that dictate stacking interaction[2c,f] is relatively unknown. Stronger charge-transfer process in the stacking interaction can be distinguished by the CT band in the absorption spectroscopy, while the electrostatic interactions cannot be easily quantified and are often difficult to diagnose. Some qualitative understanding, however, has been developed by observation of the steric proximity in the X-ray crystal structure analysis[2g] or by diamagnetic shielding/deshielding of specific protons upon stacking as observed in the NMR spectroscopy[2h,i] as well as by computational methods[2f] in both biological and nonbiological systems.

Several attempts have been made to show stacking (both by NMR and X-ray crystallography) in both biological[2a,b,h,i] as well as nonbiological systems.[2c−e,3a,4,8] The tools used so far are the concentration- and temperature-dependent studies by UV, CD, or ORD,[2b] as well as the relative shielding/deshielding and/or NOE contacts

[†] Uppsala University.
[‡] Ochanomizu University.

(1) (a) Jeffrey, G. A.; Saenger, W. *Hydrogen Boding in Biological Systems*; Springer-Verlag: Berlin, 1991. (b) Kool, E. T. *Annu. Rev. Biochem.* **2002**, *71*, 191.

(2) (a) Kool, E. T. *Annu. Rev. Biophys. Biomol. Struct.* **2001**, *30*, 1. (b) Warshaw, M. M.; Tinoco, I. Jr. *J. Mol. Biol.* **1965**, *13*, 54. (c) For reviews on aromatic interactions, see: Hunter, C. A.; Lawson, K. R.; Perkins, J.; Urch, C. J. *J. Chem. Soc., Perkin Trans. 2* **2001**, 651 and references therein. (d) Carver, F. J.; Hunter, C. A.; Seward, E. M. *J. Chem. Soc., Chem. Commun.* **1998**, 775. (e) Breault, G. A.; Hunter, C. A.; Mayers, P. C. *J. Am. Chem. Soc.* **1998**, *120*, 3402. (f) Hunter, C. A.; Sanders, J. K. M. *J. Am. Chem. Soc.* **1990**, *112*, 5525. (g) Slawin, A. M. Z.; Spencer, N.; Stoddart, J. F.; Williams, D. J. *J. Chem. Soc., Chem. Commun.* **1987**, 1070. (h) Itahara, T. *J. Chem. Soc., Perkin Trans. 2* **1998**, 1455. (i) Davis, R. C.; Tinoco, I. Jr. *Biopolymers* **1968**, *6*, 223.

(3) (a) Yamada, S.; Morita, C. *J. Am. Chem. Soc.* **2002**, *124*, 8184. (b) pK_a of the pyridinium moiety in nicotinic acid (4.68), 3-acetylpyridine (3.18), 3-chloropyridine (2.84), 3-cyanopyridine (3.71). See: Albert, A.; Serjeant, E. P. *The determination of ionization constants*; London, 1971.

10.1021/jo026572e CCC: $25.00
Published on Web 01/28/2003

by NMR.[2h,i] Stoddart et al.[2g] first identified the edge-to-face interaction in the collapsed empty cavities of crown ethers from solid-state structures. The direct experimental evidences of intramolecular stacking in solution state have come from temperature-dependent NMR studies of side-chain substituted dibenzodiazocine derivatives, concentration-dependent ^{1}H NMR studies of bis-adenine with aliphatic linker,[8b] syn/anti epimerization by temperature-dependent NMR of 1,8-diarylnaphthalene,[8f] and dynamic NMR studies of substituted benzyl pyridinium bromide,[8a] where the rotational free energy of the model aromatic systems has been quantified by NMR to show that the edge-to-face aromatic interaction as well as CH$-\pi$ interactions are the driving forces for the observed conformational isomerism. Further, the ^{1}H NMR and solid-state studies of molecular zipper complex and metal tris-bipyridine complex,[2d] as well as evaluation of NH$-\pi$ interaction-driven intermolecular association by NMR,[9c] showed the influence of such aromatic interactions in bimolecular complex formation.

Results and Discussion

Yamada et al. have demonstrated[3a] that it is possible to selectively shield one side of the pyridinium face by the intramolecular stacking of the neighboring phenyl ring in a nicotinamide derivative (as in **1a**), which allows

(4) Cation$-\pi$ interaction: (a) Gallivan, J. P.; Dougherty, D. A. *Proc. Natl. Acad. Sci. U.S.A.* **1999**, *96*, 9459. (b) For review: Ma, J. C.; Dougherty, D. A. *Chem. Rev.* **1997**, *97*, 1303 and references therein. (c) Wolf, R.; Asakawa, M.; Ashton, P. R.; Gómez-López, Hamers, C.; Menzer, S.; Parsons, I. W.; Spencer, N.; Stoddart, J. F.; Tolley, M. S.; Williams, D. J. *Angew. Chem., Int. Ed.* **1998**, *37*, 1433. (d) Lämsä, L.; Huuskonen, J.; Rissanen, K.; Pursiainen, J. *Chem. Eur. J.* **1998**, *4*, 84. (e) Ashton, P. R.; Philip, D.; Spencer, N.; Stoddart, J. F.; Williams, D. J. *J. Chem. Soc., Chem. Commun.* **1994**, 181. (f) Balzani, V.; Credi, A.; Mattersteig, G.; Mattews, O. A.; Raymo, F. M.; Stoddart, J. F.; Venturi, M.; White, A. J. P.; Williams, D. J. *J. Org. Chem.* **2000**, *65*, 1924. (g) Ortholand, J.-Y.; Slawin, A. M. Z.; Spencer, N.; Stoddart, J. F.; Williams, D. J. *Angew. Chem., Int. Ed. Engl.* **1989**, *28*, 1394. (h) Amabilino, D. B.; Ashton, P. R.; Boyd, S. E.; Lee, J. Y.; Menzer, S.; Stoddart, J. F.; Williams, D. J. *Angew. Chem., Int. Ed. Engl.* **1997**, *36*, 2070. (i) Allwood, B. L.; Shahriari-Zavareh, H.; Stoddart, J. F.; Williams, D. J. *J. Chem. Soc., Chem. Commun.* **1987**, 1058. (j) Lämsä, L.; Suorsa, T.; Pursiainen, J.; Huuskonen, J.; Rissanen, K. *J. Chem. Soc., Chem. Commun.* **1996**, 1443. (k) Philip, D.; Slawin, A. M. Z.; Spencer, N.; Stoddart, J. F.; Williams, D. J. *J. Chem. Soc., Chem. Commun.* **1991**, 1584.

(5) The sign for $\Delta\delta^{H}_{N-P}$ and $\Delta\Delta\delta^{H}_{N-P}$ (in ppm) corresponds to the relative shielding (upfield shift, $\Delta\delta$ or $\Delta\Delta\delta > 0$) or deshielding (downfield shift, $\Delta\delta$ or $\Delta\Delta\delta < 0$) as a function of pH.

(6) (a) The intra- and intermolecular stacking and/or other aromatic interactions [2a,c,f,h,6b,d,e,8f] involving both biological as well as nonbiological systems are a topic of fundamental interest related to molecular recognition and biological functionalities. Several types of noncovalent aromatic interactions have been identified so far such as aryl$-\pi$,[6f] alkyl$-\pi$[6f] or commonly CH$-\pi$,[9b] cation$-\pi$,[4a,b] anion$-\pi$,[6g] polar/π,[6d,8f] and charge-transfer processes.[2f,6b] *Whether such interactios are mediated by electrostatics or charge-transfer interaction is still a major debate.* The general trend of identifying the charge-transfer complex is to observe the characteristic UV charge-transfer band (in the exited state involving $\pi-\pi^*$, n$-\pi^*$, or $\sigma-\pi^*$ transitions). According to Kool et al.,[2a,6e] aromatic stacking interaction between nucleobases in water involves electrostatics (dipole−dipole and dipole−induced dipole) interactions, dispersion (momentary dipole−induced dipole) effects, and solvation. Hunter et al.[2c,f] invoked offset stacking involving attractive atom$-\pi\sigma$ interaction (electrostatic in nature) and edge-to-face interactions, rather than repulsive $\pi-\pi$ interaction as in face-to-face stacking between two aromatic moieties. Dougherty et al.[4a,b] showed that electrostatic and polarization effects are the dominant contributions in the cation$-\pi$ interaction. However, the quadrupole moment[4b] and dispersion effect of aromatic system as well as charge transfer interaction occasionally play a secondary role in such processes. Theoretical studies[6f] recently showed that dispersion effects other than electrostatics dominate both aryl CH$-\pi$ and alkyl CH$-\pi$ interactions. In all cases, alkyl CH$-\pi$ interactions are weaker than aryl CH$-\pi$ interactions. Nishio et al.[9a,b] proposed partial charge-transfer arising from through-space proximity between alkyl hydrogen and aromatic moiety as the basis for CH$-\pi$ interaction. On the other hand, Siegel et al.[6d,8f] and Diedrich et al.[6d] invoked a through-space polar (Coulombic)/π contribution as a dominating factor over the charge-transfer process for the aromatic interaction involving substituted 1,8-diarylnaphthalene where there is no UV charge-transfer band observed. However, Inoue et al.[6b] cited examples of *ground-state partial charge transfer* process in intra- and intermolecular stacking involving indole and adeninium rings. It has also been presumed that the partial charges distribution of two nearest neighbor aromatic systems play important role in their donor−acceptor properties,[6b] thereby having impact in the pK_a perturbation.[6h] (b) Ishida, T.; Shibata, M.; Fuji, K.; Inoue, M. *Biochemistry* **1983**, *22*, 3571. (c) Schmidt, A.; Kindermann, M. K.; Vainotalo, P.; Nieger, M. *J. Org. Chem.* **2000**, *64*, 9499. (d) Cozzi, F.; Cinquini, M.; Annuziata, R.; Dwyer, T.; Siegel, J. S. *J. Am. Chem. Soc.* **1992**, *114*, 5729. (e) Guckian, K. M.; Schweitzer, B. A.; Rex, X.-F.; Charles, J. S.; Tahmassebi, D. C.; Kool, E. T. *J. Am. Chem. Soc.* **2000**, *122*, 2213. (f) Ribas, J.; Cubero, E.; Luque, J.; Orozco, M. *J. Org. Chem.* **2002**, *67*, 7057 and references therein. (g) Quiñonero, D.; Garau, C.; Rotger, C.; Frontera, A.; Ballester, P.; Costa, A.; Deyà, P. M. *Angew. Chem., Int. Ed.* **2002**, *41*, 3389. (h) Narlikar, G. J.; Herschlag, D. *Annu. Rev. Biochem.* **1997**, *66*, 19 and references therein.

(7) (a) The comparison of the crystal structures (Supporting Information in ref 2) for **1a** and **1b** showed that in the later, the pyridinium and phenyl rings are stacked face-to-face (with distance between them ∼3.4 Å), whereas in the former, pyridinyl and phenyl moieties are apart. It is evident from the conformational comparison for abovementioned crystal structures of neutral **1a** and methylated **1b** that rotation of ∼100° around the C2−C10 bond [i.e. through the $\Phi_{[C3-C2-C10-C11]}$ and $\Phi_{[N1-C2-C10-C11]}$ where Φ represents the dihedral angle] in **1a** (∼80° and −168°, respectively) cause a rotation of the phenyl ring to form a face-to-face stacking with the neighboring pyridinium ring, as found in the X-ray of **1b** (∼178° and −68°, respectively). However, in the typical Karplus curve the change of 90° in dihedral cause minimal (almost zero) changes in exocylic $^3J_{H,H}$, thus our ^{1}H NMR analyses at 298 K of an aqueous solution of neutral (N) **1a** (pH = 6.7) and methylated **1b** or protonated (P) **1a**$^+$ (pH = 1.05) have not shown any appreciable change of $^3J_{H,H}$ as a function of pH [$^3J_{H2A,H10B} = 0$ Hz for both N and P state; $^3J_{H2A,H10A} = 4.9$ and 4.7 Hz for N and P states, respectively; $^3J_{H2A,H3A} = 6.2$ and 5.0 Hz for N and P states, respectively; $^3J_{H2A,H3B} = 8.4$ and 10.2 Hz for N and P states, respectively, Table 2]. Hence, it is not possible to determine the exact solution structures of **1a**, **1b** or protonated **1a**$^+$. So the relative chemical shift changes ($\Delta\delta_{N-P}$, vide infra) in the titration profile of **1a** → **1a**$^+$, showed an edge-to-face overlap of pyridinium moiety with phenyl group in **1a**$^+$ [*because of nonuniform shielding among pyridinyl protons (vide infra) suggesting that H5/H9 edge of pyridinyl moiety is more in contact with the phenyl than the H7/H8 edge*] in contrast to the solid-state structure of **1b**. (b) How do we distinguish an interaction such as CH$-\pi$ interaction from the simple NMR deshielding influence? Deshielding of a proton suggests that it is within the diamagnetic anisotropy of the phenyl ring current, which means that the proton is interacting with the ring-current by either CH$-\pi$ interaction such as between methyl and phenyl or in a cation$-\pi$ interaction between phenyl and pyridinyl system. The real evidence of this CH-π interaction is that it is tunable by conformational changes, which is *driven* by electrostatics of the pyridinium$-\pi$ (phenyl) interaction, and the resulting electronic environment of the phenyl group in **1a**$^+$. The proof is that we get the pK_a of pyridine from the pH-dependent chemical shifts of both methyl groups, which shows that the whole pyridine-phenyl-methyl system is indeed coupled—one cross-modulates the other in tandem by using the electrostatic as the engine, and the origin of this electrostatics is a far away point in the molecule—the pyridinyl-nitrogen.

(8) (a) Rashkin, M. J.; Waters, M. L. *J. Am. Chem. Soc.* **2002**, *124*, 1860. (b) Newcomb, L. F.; Gellman, S. H. *J. Am. Chem. Soc.* **1994**, *116*, 4993. (c) The experimental evidence showed that the magnitude of offset edge-to-face stacking interactions is dictated by the geometry of the stacked components, which, in turn, is influenced by the nature of ring substituents. Kim, E.; Paliwal, S.; Wilcox, C. S. *J. Am. Chem. Soc.* **1998**, *120*, 11192. (d) Paliwal, S.; Geib, S.; Wilcox, C. S. *J. Am. Chem. Soc.* **1994**, *116*, 4497. (e) Jennings, W. B.; Farrell, B. M.; Malone, J. F. *Acc. Chem. Res.* **2001**, *34*, 885. (f) Cozzi, F.; Cinquini, M.; Annuziata, R.; Siegel, J. S. *J. Am. Chem. Soc.* **1993**, *115*, 5330. (g) A geometrical dependence on aromatic interaction has been observed in flavoenzyme mimic: Goodman, A. J.; Breinlinger, E. C.; McIntosh, C. M.; Grimaldi, L. N.; Rotello, V. M. *Org Lett.* **2001**, *3*, 1531.

(9) (a) A database study of CH$-\pi$ interaction: Umezawa, Y.; Tsuboyama, S.; Takahashi, H.; Uzawa, J.; Nishio, M. *Tetrahedron* **1999**, *55*, 10047 and references therein. (b) Suezawa, H.; Hashimoto, T.; Tsuchinaga, K.; Yoshida, T.; Yuzuri, T.; Sakakibara, K.; Hirota, M.; Nishio, M. J. *J. Chem. Soc., Perkin Trans. 2* **2000**, 1243. (c) Snowden, T. S.; Bisson, A. P.; Anslyn, E. V. *J. Am. Chem. Soc.* **1999**, *121*, 6324.

SCHEME 1. All Compounds (1a and 2a) along with Their Protonated (1a$^+$ and 2a$^+$) and Methylated (1b and 2b) Analogues Used in These NMR Studies[a]

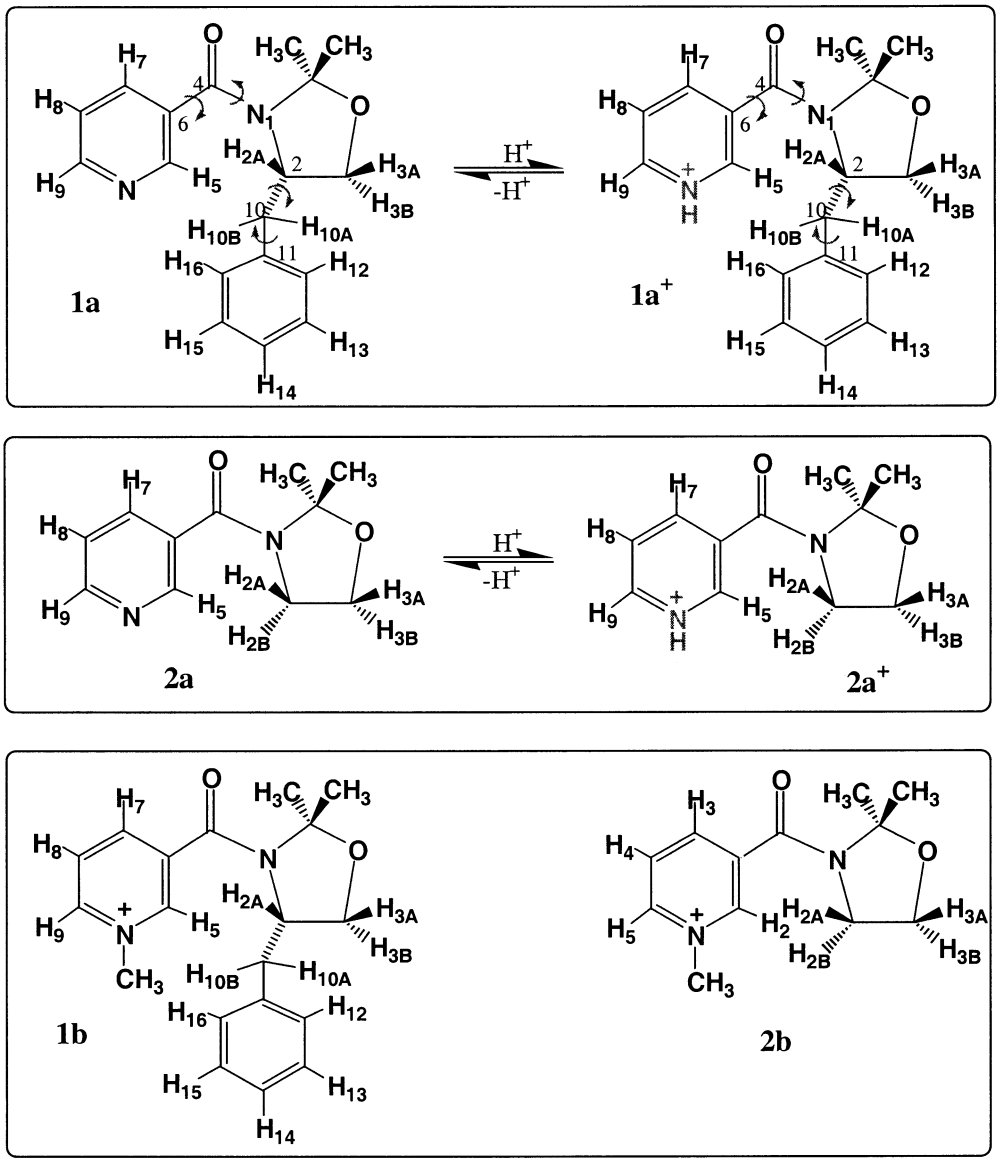

[a] Numbering of protons has been done according to the ORTEP drawing of the corresponding crystal structure given in the Supporting Information of ref 3a. The arrows across different torsions in **1a** and **1a**$^+$ show that mainly by rotating through these torsions these molecules can adopt various stacking geometries.

nucleophiles to attack only from the nonshielded side to give exclusively 1,4-adduct over the 1,6-adduct in 99% ee. These authors have evidenced face-to-face stacking in the solid state by X-ray crystallography. It is, however, not possible to determine their exact solution structures because of the low proton density across the torsions (shown for **1a** and **1a**$^+$ in Scheme 1) through which intramolecular rotation takes place to interconvert among various possible stacking geometries.[7a] We herein show that our pH titration method constitutes a powerful means to shed light on the nature and geometry of the intramolecular interactions provided the complex has a protonation or a deprotonation site as in compound **1a**.

A. The pH Titration of the Protons of the Pyridinyl Group Shows That Its Basicity Is Tunable Owing to the Interactions with the Nearest Neighbors. Our systematic pH titration studies by ^{1}H NMR spectroscopy of **1a** → **1a**$^+$ in comparison with the standard **2a** → **2a**$^+$ (Scheme 1) reveals that the intramolecular stacking interaction is indeed edge-to-face in the aqueous solution, not face-to-face. We also show that the basicity of the pyridinyl group (pK_a 2.9) in **1a** can be measured not only from the pH-dependent chemical shifts of the pyridinyl protons but also from the protons of the neighboring phenyl (pK_a 2.92) and methyl (pK_a 3.07) groups as a result of intramolecular stacking owing to the electrostatic interaction among the nearest neighbors at the ground state.

Thus, the pH-dependent titration of **1a** gave a typical sigmoidal titration curve to show the formation of the protonated (P) **1a**$^+$ (panels A−D in Figure 1). The transformation **1a** → **1a**$^+$ showed only the upfield shift of δH5 ($\Delta\delta_{N-P}^{H5(py)}$: 0.029), and all other pyridinyl (py)-

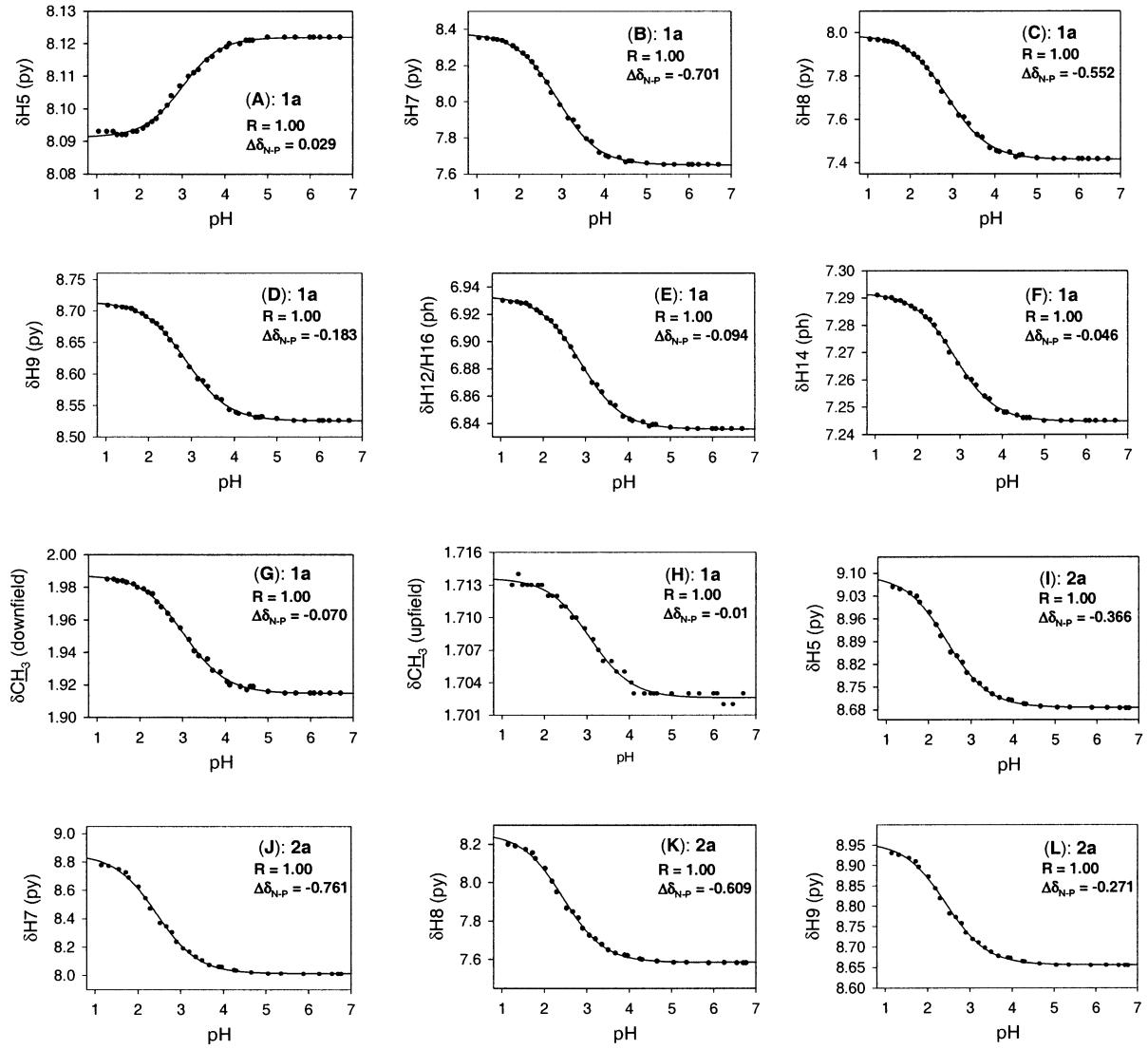

FIGURE 1. (A−H) pH-dependent ^{1}H chemical shifts (py and/or ph in parentheses stand for pyridinyl and phenyl moieties, respectively) of **1a** [A, δH5 (py); B, δH7 (py); C, δH8 (py); D, δH9 (py); E, δH12/H16 (ph); F, δH14 (ph); G, δCH_3 (downfield); H, δCH_3 (upfield)] within the pH range 1.04 ≤ pH ≤ 6.7. (I−L) pH-dependent ^{1}H chemical shifts of **2a** [I, δH5 (py); J, δH7 (py); K, δH8 (py); L, δH9 (py)]. R denotes the Pearson correlation coefficient of the nonlinear fit.

protons showed the downfield shifts: $\Delta\delta_{N-P}^{H7(py)}$, −0.701; $\Delta\delta_{N-P}^{H8(py)}$, −0.552; $\Delta\delta_{N-P}^{H9(py)}$, −0.183 (Table 1). Subsequent Hill plot analyses (panels a−d in Figure 2) gave the pK_a of 3.06 ± 0.02 from δH5, 2.93 ± 0.01 from both δH7 and δH8, and 2.92 ± 0.01 from δH9. A similar pH-dependent titration of the standard **2a** (panels **I**−**L** in Figure 1) gave **2a**$^+$ also showing sigmoidal titration curve, in which the chemical shifts of all pyridinyl protons move downfield: $\Delta\delta_{N-P}^{H5(py)}$, −0.366; $\Delta\delta_{N-P}^{H7(py)}$, −0.761; $\Delta\delta_{N-P}^{H8(py)}$, −0.609; $\Delta\delta_{N-P}^{H9(py)}$, −0.271 (Table 1). A Hill plot analysis (panels **i**−**l** in Figure 2) subsequently showed the pK_a of 2.56 ± 0.02 of the protonated form **2a**$^+$ (Table 1). The differences in relative shielding of various protons in protonated **2a**$^+$ compared to that in **1a**$^+$, with reference to their neutral counterparts **2a** and **1a**, show that the pyridinyl protons are shielded[5] in the order δH5 ($\Delta\Delta\delta_{N-P}^{H5(py)}$ = 0.397 ppm) > δH9 ($\Delta\Delta\delta_{N-P}^{H9(py)}$ = 0.088 ppm) > δH7 ($\Delta\Delta\delta_{N-P}^{H7(py)}$ = 0.061 ppm) ≈ δH8 ($\Delta\Delta\delta_{N-P}^{H8(py)}$ = 0.057 ppm), where $\Delta\Delta\delta_{N-P}^{H}$ (in ppm) = $[\Delta\delta_{N-P}^{H}]_{\mathbf{2a}\rightarrow\mathbf{2a}^+}$ − $[\Delta\delta_{N-P}^{H}]_{\mathbf{1a}\rightarrow\mathbf{1a}^+}$. This demonstrates that the H5/H9-edge of the pyridinyl group is more affected than the H7/H8-edge (Scheme 1) from the neighboring phenyl ring, which constitutes a direct evidence of an edge-to-face cation (pyridinium)−π (phenyl) interaction[3a,4,7a] in the aqueous solution. It should however be noted that the reported shielding tendency for the N-methylated analogue **1b** in $CDCl_3$ is very different[3a] from those found in the aqueous solution, suggesting that its geometry is significantly dictated by the solvent effect.

B. The pH Titration of the Pyridinyl Protons Gives a Quantitative Measurement of the Intramolecular Electrostatic Charge Transfer from the Neighboring Phenyl to the Pyridinyl (Pyridinium) Group. Interestingly, the electrostatic charge enrichment[6a,b] of the electron-deficient pyridinyl ring owing to the presence of the neighboring electron-rich phenyl (ph) ring is also evident by the relative deshielding of δH12/

TABLE 1. pK_a, Free Energy of Protonation (ΔG^o_{pKa})[a], ^{1}H Chemical Shift Difference, Spin−Lattice (T_1, ΔT_1, and $\Delta T_1^{\neq}$) between the Neutral (N) and the Protonated (P) States ($\Delta\delta_{N-P}$)[b] of Aromatic Protons of Pyridinium and Phenyl Moieties as Well as that of Methyl Groups of 1a and 2a at 298 K at 500 MHz.

	pyridinyl (pyridinium) moiety								phenyl moiety				methyl group[c]			
	δH5		δH7		δH8		δH9		δH12/H16		δH14		downfield		upfield	
	1a	**2a**	**1a**	**2a**	**1a**	**2a**	**1a**	**2a**	**1a**	**2a**	**1a**	**2a**	**1a**	**2a**	**1a**	**2a**
pK_a [d]	3.06 (±0.02)	2.56 (±0.02)	2.93 (±0.01)	2.56 (±0.02)	2.93 (±0.01)	2.56 (±0.02)	2.92 (±0.01)	2.55 (±0.02)	2.92 (±0.01)	*e*	2.90 (±0.01)	*e*	3.07 (±0.02)	*f*	3.10 (±0.02)	*f*
ΔG^o_{pKa}	17.5 (±0.1)	14.6 (±0.1)	16.7 (±0.1)	14.6 (±0.1)	16.7 (±0.1)	14.6 (±0.1)	16.7 (±0.1)	14.5 (±0.1)	16.7 (±0.1)	*e*	16.5 (±0.1)	*e*	17.5 (±0.1)	*f*	17.7 (±0.1)	*f*
$\Delta\delta_{N-P}$	0.029	−0.366	−0.701	−0.761	−0.552	−0.609	−0.183	−0.271	−0.094	*e*	−0.046	*e*	−0.070	*f*	−0.010	*f*
T_1 (N) [h]	3.1	12.3	1.9	4.9	2.1	5.4	3.3	8.9	2.2	*e*	2.4	*e*	0.9	*i*	0.8	*i*
T_1 (P)[h]	3.8	8.5	1.9	4.2	2.4	4.1	3.9	7.8	2.3	*e*	2.5	*e*	0.9	*i*	0.9	*i*
ΔT_1 (N) [j]	9.2		3.0		3.3		5.5		*k*	*e*	*k*	*e*	1.3		0.9	
$\Delta T_1^{\neq}$ (P) [j]	4.7		2.3		1.7		3.9						1.3		0.8	

[a] In kJ mol^{-1}; see ref 10 for details. [b] In ppm. The sign for $\Delta\delta_{N-P}$ corresponds to the relative shielding (upfield shift, $\Delta\delta > 0$) or deshielding (downfield shift, $\Delta\delta < 0$) as a function of pH [N for neutral state (pH = 6.7; **1a** or **2a**) and P for protonated state (pH = 1.05; **1a**$^+$ or **2a**$^+$)]; see Figure 1 and ref 5. [c] Methyl groups are bonded to the 2,2-dimethyloxazolidine moiety; see Scheme 1. For **2a**, both methyl resonances are isochronous. However, two non-isochronous methyl protons in **1a** (or **1a**$^+$) are shifted downfield and upfield with respect to that of **2a** (or **2a**$^+$). [d] pK_a values have been calculated using Hill plots (see Figure 2). [e] No phenyl moiety present in **2a**. [f] No observed sigmoidal change of chemical shift over the pH range studied. Thus, no pK_a values and corresponding free energy of protonation have been calculated. [g] Insignificant change or almost no change of chemical shift (<0.002 ppm) over the pH range studied. [h] The spin−lattice relaxation time T_1 (±10%)[12a] was calculated (in seconds) by using intensity and area fits with the aid of Bruker software using inversion−recovery technique. The T_1 (N) and T_1 (P) signify the T_1 for the neutral state (N) and the protonated state (P). See the Experimental Section for details of T_1 calculation. [i] In the case of **2a**, the two methyl protons in both neutral and acidic pH are isochronous. The measured T_1 at neutral and protonated state are 2.2 s and 1.7 s, respectively. [j] The ΔT_1 and $\Delta T_1^{\neq}$(in seconds) are measured as $[T_1]_{\mathbf{2a}} - [T_1]_{\mathbf{1a}}$ for the neutral (N) state and $[T_1]_{\mathbf{2a}^+} - [T_1]_{\mathbf{1a}^+}$ for the protonated (P) state, respectively, to show the relative relaxation rate of each proton using the protons of **2a** as standard. [k] No phenyl protons in **2a**, hence, not calculated.

H16 as well as that of δH14 ($\Delta\delta^{H12/H16(ph)}_{N-P} = -0.094$ and $\Delta\delta^{H14(ph)}_{N-P} = -0.046$, Table 1) of the phenyl ring in protonated **1a**$^+$ compared to that in the neutral **1a**. Further evidence of this intramolecular interaction between pyridinium and phenyl moieties comes from the fact that the pK_a for the protonation of pyridinyl-nitrogen of **1a** can also be monitored from the pH-dependent sigmoidal downfield shifts (panels E and F in Figure 1) and subsequent Hill plot analysis (panels e and f in Figure 2) of the phenyl protons: δH12/H16 (pK_a: 2.92 ± 0.01) and δH14 (pK_a: 2.90 ± 0.01). Clearly, it is the ortho/para activating effect at C12/C16 and C14 centers (see Scheme 1) of the phenyl ring, owing to the methylene group, that results in partial charge donation[6a] to the electron-deficient pyridinium group, whereas the H13/H15 protons at the meta centers remain nonresponding.

C. Evidence for the Cross-Talk between Pyridinyl (Pyridinium) and the Neighboring Phenyl Groups by Electrostatic Charge-Transfer Interaction. The absence of any orbital interaction[8f] has already been evidenced by Yamada et al.[3a] by showing the absence of *charge-transfer band in UV for **1b*** (a methylated analogue of **1a**$^+$). Thus, it is very likely that the electrostatics play a major role[6a] in the stabilization of such edge-to-face interaction between the pyridinium (cation) and the phenyl (π) groups,[4a] in which the attractive Coulombic term[6d,8f] should be dominant between the electron-deficient pyridinium and electron-rich phenyl groups. However, a simple chemical shift argument ($\Delta\delta^{H}_{N-P}$, Table 1) shows that pyridinium δH5 is moving upfield [$\Delta\delta^{H5(py)}_{N-P}$: 0.029] in **1a** compared to that in **2a**, where all phenyl protons of **1a** are moving downfield (Table 1).

Moreover, all pyridinium protons in **1a** also showed relative upfield shifts (**(**$\Delta\Delta\delta^{H}_{N-P}$, Table 1) compared to those in the standard **2a**. These observations suggest that a partial charge transfer[6a] from the neighboring phenyl ring to the pyridinium system is most probably taking place in **1a** and **1a**$^+$, as opposed to "purely polar effects"[6d] assumed in the molecular complexation in disubstituted naphthalenes.

However, the net result of this nearest neighbor interaction between the phenyl moiety and pyridinium ion is that the pyridinium moiety in **1a**$^+$ has become more basic (pK_a 2.92) compared to that in the standard **2a**$^+$ (pK_a 2.56) as a consequence of edge-to-face[2c,f,g,8a−f] electrostatic interaction rather than face-to-face[7a] aromatic stacking through the stabilization of pyridinium (cation) and the phenyl (π) interaction by charge transfer.[4] This is equivalent to a ΔpK_a of 0.36 (Table 1), which amounts to additional free-energy stabilization ($\Delta\Delta G^o_{pKa}$)[10c] of −2.1 kJ mol^{-1} for the cation (pyridinium)−π (phenyl) interaction. The above observations thus constitute a direct evidence of the charge transfer through space between electron-rich and electron-deficient systems by electrostatics at the ground state.

D. Cascade of Intramolecular Electrostatic Interactions at the Ground State Giving the Pyridinium−Phenyl−Methyl Cross-Talk. In this context, it is interesting to note that the two nonisochronous methyl protons of the 2,2-dimethyloxazolidines in **1a** also showed the pH-dependent sigmoidal titration curve as **1a**$^+$ is formed as a result of CH (methyl)−π (phenyl) interaction,[7b] which is orchestrated by the protonation of the pyridinyl-nitrogen (panels G and H in Figure 1 for titration plots and panels g and h in Figure 2 for corresponding Hill plots). Thus, the pK_a of the pyridinyl

(10) (a) Perrin, D. D.; Dempsey, B.; Serjeant, E. P. *pK_a Prediction for Organic Acids and Bases*; Chapman and Hall: New York, 1981. (b) Sharp, K. A.; Honig, B. *Annu. Rev. Biophys. Biophys.* **1990**, *19*, 301. (c) The equation[10a, b] $\Delta G^o_{pKa} = 2.303RTpK_a$ shows the estimation of free energy (ΔG^o_{pKa}, in kJ mol^{-1}) of protonation at 298 K for compounds **1a** and **2a** (Scheme 1). So the ΔpK_a gives the estimation of $\Delta\Delta G^o_{pKa}$ (in kJ mol^{-1}). ΔpK_a for cation−π interaction is $(pK_a)_{\mathbf{2a}^+} - (pK_a)_{\mathbf{1a}^+}$ and that for CH−π interaction is (pK_a from δCH_3)$_{\mathbf{1a}^+}$ − (pK_a from δH of phenyl moiety)$_{\mathbf{1a}^+}$.

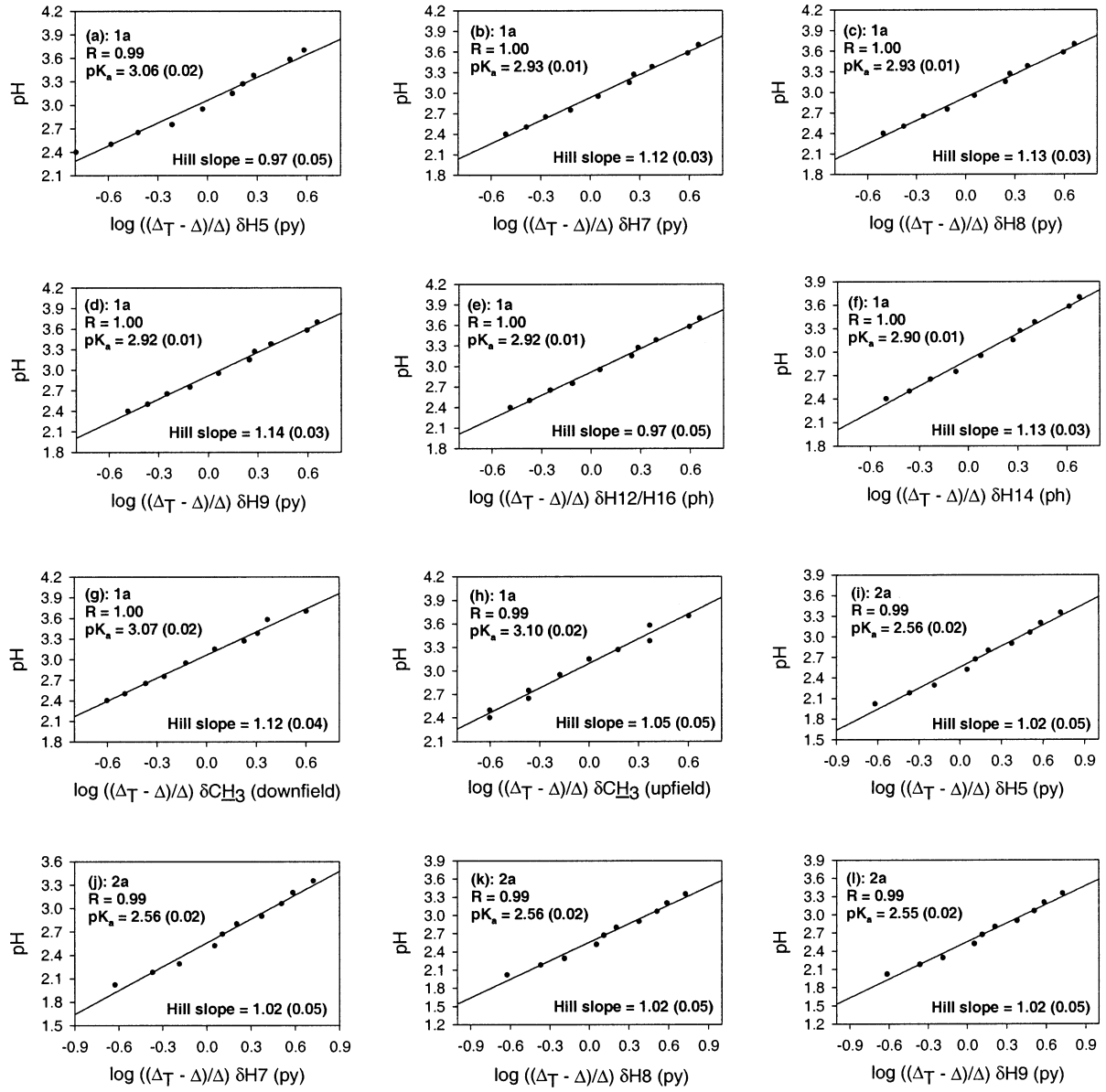

FIGURE 2. (a−l) Hill plots for each proton [plot of $\log((\Delta_{N-P} - \Delta_P)/\Delta_P)$ as a function of pH] of **1a** and **2a**. The legend of Figure 1 shows the corresponding values of Δ_{N-P} (see the Experimental Section for further details). (a−h) Hill plots for **1a** [a, δH5 (py); b, δH7 (py); c, δH8 (py); d, δH9 (py); e, δH12/H16 (ph); f, δH14 (ph); g, δCH_3 (downfield); h, δCH_3 (upfield)] within the pH range $1.04 \leq$ pH ≤ 6.7 (py and/or ph in parentheses stand for pyridinyl and phenyl moieties, respectively). (i−l) Hill plots for **2a** [i, δH5 (py); j, δH7 (py); k, δH8 (py); l, δH9 (py)]. The linear fit of each plot (R denotes the Pearson correlation coefficient) gives the corresponding Hill slope and pK_a (the error is in parentheses).

group measured from the pH-dependent titration of the downfield methyl protons is found to be 3.07 ± 0.02 with $\Delta\delta_{N-P}^{CH3}$ −0.07, whereas the upfield methyl protons gave the pK_a of 3.10 ± 0.02 with $\Delta\delta_{N-P}^{CH3}$ −0.01.

The chemical shift of a C*H*-proton involved in the CH−π interaction[9a] is known to move upfield,[9b] because of shielding from the π cloud owing to the partial charge-transfer interaction.[9b] However, both the non-isochronous methyl protons (δCH_3) in **1a** move downfield[7b] ($\Delta\delta_{N-P}^{CH3} <$ 0, see Table 1) as a function of pH.

The reason for this is as follows: The protonation of the pyridine moiety (i.e., formation of pyridinium cation at acidic pH) promotes the partial charge tarnsfer[6a] from the neighboring phenyl (π) moiety to the electron-deficient pyridinium in **1a**$^+$, thereby causing the charge depletion at the phenyl moiety, which in turn reduces the strength of the CH (methyl)-π (phenyl) interaction as the pyridinium ion is formed. This means that the pyridinium cation acts as electron withdrawing substituent, an electron pump, on the phenyl ring simply owing to their spatial proximity. Such an effect of the aromatic substituent on the strength of the CH−π interaction has been reported previously.[9b]

The above pH-dependent downfield shift ($\Delta\delta_{N-P}^{CH3} < 0$, Table 1) of the methyl group therefore suggests that the CH (methyl)−π (phenyl) interaction is *strongest at around the neutral pH*, and this interaction is gradually diminished as the pyridinium cation is formed.

Similarly, the comparison of chemical shifts (Table 2) for the pyridinyl protons at the neutral (N) state for **1a**

TABLE 2. ^{1}H Chemical Shift of Aromatic Protons of Pyridinyl/Pyridinium and Phenyl Moieties of 1a$^+$ Compared to 1b as Well as in 2a$^+$ Compared to that of 2b at 298 K (^{1}H NMR Derived $^3J_{HH}$ and $^2J_{HH}$ at 298 K for 1a at the Protonated (1a$^+$, pH = 1.05) and the Neutral (1a, pH = 6.70) States)

		δ_H (in ppm) of pyridinium moiety[a]				δ_H (in ppm) of phenyl moiety[b]			$^3J_{H,H}$[c] (in Hz)				$^2J_{H,H}$[d] (in Hz)	
compd	pH	δH5	δH9	δH7	δH8	δH14	δH13/H15	δH12/H16	I	II	III	IV	V	VI
1a	6.70	8.122	8.526	7.651	7.417	7.245	7.176	6.836	8.4	6.2	4.9	0.0	9.2	13.7
1a$^+$	1.04	8.093	8.709	8.352	7.969	7.291	7.180	6.929	10.2	5.0	4.7	0.0	9.0	13.8
1b		8.091	8.699	8.339	7.948	7.368	7.202	6.957	9.4	4.3	5.0	0.0	9.2	13.4
2a	6.70	8.685	8.655	8.010	7.582	*e*	*e*	*e*	*f*	*f*	*f*	*f*	*f*	*f*
2a$^+$	1.04	9.051	8.926	8.771	8.191	*e*	*e*	*e*	*f*	*f*	*f*	*f*	*f*	*f*
2b		9.097	8.931	8.710	8.179	*e*	*e*	*e*	*f*	*f*	*f*	*f*	*f*	*f*

[a,b] ^{1}H NMR in D_2O at 298 K; see the Experimental Section for details and Scheme 1 for atom numbering. [c,d] The $^3J_{H,H}$ corresponding to I−VI are as follows: I, $^3J_{H2A,H3B}$; II, $^3J_{H2A,H3A}$; III, $^3J_{H2A,H10A}$; IV, $^3J_{H2A,H10B}$; V, $^2J_{H10A,H10B}$; VI, $^2J_{H3A,H3B}$. [e] No phenyl group present. [f] Not calculated.

TABLE 3. Calculated Energies (HF 6-31G) and Energy Differences for Protonated and Neutral Nicotinamide Derivatives (1a, 1a$^+$, 2a, and 2a$^+$), as Well as Their Respective Dipole Moments**

	1a	**1a**$^+$	$(\Delta_{\mathbf{1a}^+} - \Delta_{\mathbf{1a}})$[1]	**2a**	**2a**$^+$	$(\Delta_{\mathbf{2a}^+} - \Delta_{\mathbf{2a}})$[a]
HF energy (au)	−951.938236	−952.318095	−238.37[1]	−683.346941	−683.723011	−235.99[a]
$\Delta G°_g$ (kcal mol^{-1})	205.47[b]	214.74[b]	9.27	136.64[b]	145.82[b]	9.18
$\Delta H°_g$	247.50	256.69		170.52	179.80	
$-T\Delta S°_g$	−42.03	−41.95		−33.88	−33.98	
$\Delta G°_{sol}$ (kcal mol^{-1})						
IEFPCM[14a]	−5.67	−52.54	−46.87	−8.14	−58.13	−49.99
COSMO[14b]	−5.82	−52.22	−46.40	−8.36	−57.91	−49.55
PCM[15]	−4.63	−51.24	−46.61	−8.22	−57.48	−49.26
proton affinities[c]	-		229.08	-		226.7
dipole moment						
(gas phase)	2.543	12.714		2.468	10.843	
(solution phase)	3.591	14.988		3.080	12.969	

[a] In kcal mol^{-1}. [b] For the individual compounds, the $\Delta G°_g$ shown are the sums of thermal free energies ($\Delta G° = \Delta H° - T\Delta S°$) [c] Proton affinities[16] in kcal mol^{-1}.

with those of **2a** shows relative upfield shift of the protons in the former [$\Delta\delta H^N$ (in ppm) > 0, where $\Delta\delta H = \delta H_{\mathbf{2a}} - \delta H_{\mathbf{1a}}$]. This suggests that the electron-deficient pyridinyl and electron-rich phenyl moieties in **1a** have CH (pyridinyl)−π (phenyl) interaction[6f,9] *even in the neutral state* ($\Delta\delta H5^N$, 0.563; $\Delta\delta H7^N$, 0.359; $\Delta\delta H8^N$, 0.165; $\Delta\delta H9^N$, 0.129).

On the other hand, a comparison of the chemical shifts (Table 2) at the protonated (P) state for **1a**$^+$ with those of **2a**$^+$ [i.e. $\Delta\delta H^P$ (in ppm) > 0, where $\Delta\delta H = \delta H_{\mathbf{2a}^+} - \delta H_{\mathbf{1a}^+}$] shows relative upfield shift of the protons in the former, suggesting the presence of the cation−π interaction[4] ($\Delta\delta H5^P$, 0.958; $\Delta\delta H7^P$, 0.419; $\Delta\delta H8^P$, 0.222; $\Delta\delta H9^P$, 0.217).

Thus, a comparison between $\Delta\delta H^N$ and $\Delta\delta H^P$ clearly shows that the CH (pyridinyl)−π (phenyl) interaction[6f,9] in the *neutral state* in **1a** is relatively weaker than the cation (pyridinium)−π (phenyl) interaction[4] in **1a**$^+$.

It has been further shown from relative chemical shift changes and the pK_a analyses[10b] that the cation (pyridinium)−π (phenyl) interaction ($\Delta G°_{cation-\pi} = -2.1$ kJ mol^{-1}) is indeed stronger than the CH (methyl)−π (phenyl) interaction ($\Delta G°_{CH-\pi} = -0.8$ kJ mol^{-1}).

That it is the neighboring phenyl, not the pyridinyl (pyridinium) moiety, which is participating in the proposed CH−π interaction with methyl protons in **1a** or **1a**$^+$ comes from the following facts: (i) The two methyl signals of the 2,2-dimethyloxazolidines in **1a** and **1a**$^+$ are non-isochronous owing to the influence of the phenyl moiety, which should be compared to their isochronous behavior in the standard **2a** or **2a**$^+$, in which the phenyl group is absent. (ii) Unlike the pH-dependent sigmoidal shift of the methyl group found during protonation of **1a** → **1a**$^+$, there is no such pH-dependent shift of the isochronous methyl protons in the protonation of the standard **2a** → **2a**$^+$, which clearly shows that the methyl protons are not experiencing any electrostatic interaction through the neighboring pyridinyl (pyridinium) group to give the observed CH−π interaction in **1a** or **1a**$^+$.

E. Spin−Lattice Relaxation (T_1) Studies. Since 1D NOE difference experiments both at the neutral and protonated state failed to show any NOE enhancement (actually our ab initio calculations showed that distances of all pyridinyl protons, even those of H5 and H9, from phenyl moiety are well above 3.5 Å, see Table 4) in **1a** or **1a**$^+$, we have herein used spin−lattice relaxation (T_1) study, as a complimentary "backup" of NOE kinetics[12a] to understand the nearest neighbor effect in **1a** and **1a**$^+$ with respect to the standard **2a** and **2a**$^+$. The T_1 for a small and/or medium-sized molecule shows the relaxation pathways for a particular proton depending upon its neighboring environment (lattice). The isolated protons can therefore be often identified from their much longer T_1 values.[12a] It is well established[12a] that fewer the pathways for a given proton to relax, the larger becomes its T_1 value. Thus, it has been shown from the T_1 measurement of the cyclobutyl methine signal that a cis proton has a shorter T_1 than for the trans, simply because

(11) *Bruker Almanac, NMR Tables*; Bruker, 1998; p 14.
(12) (a) Neuhaus, D.; Williamson, M. *The Nuclear Overhauser Effect In Structural and Conformational Analysis*; Springer-Verlag: Berlin, 1989; p 123. (b) Saunders: J. K.; Easton, J. W. In *Determination of Organic Structures by Physical Methods;* Nachod, F. C., Zuckerman, J. J., Randall, E. W., Eds.; Academic Press: New York, 1976; Vol. 6, pp 271−333.

TABLE 4. Essential Distances and Dihedrals for Gas-Phase Optimized (HF/6-31G) Protonated and Neutral Nicotinamide Derivatives (1a, 1a$^+$, 2a, and 2a$^+$)[a]**

	distances (Å)			
	1a	**1a$^+$**	**2a**	**2a$^+$**
d(H5−Ph[b)]	4.364 ± 0.503	3.659 ± 0.330		
d(H9−Ph[b)]	8.352 ± 0.499	7.608 ± 0.347		
d(H8−Ph[b)]	8.875 ± 0.521	8.259 ± 0.417		
d(H7−Ph[b)]	7.480 ± 0.592	7.023 ± 0.498		
d(H5−(Me-C17))[c]	4.329	4.518	4.170	4.286
d(H5−(Me-C18))[c]	2.880	2.938	2.889	2.886
d(H9−(Me-C17))[c]	6.169	6.473	6.002	6.272
d(H9−(Me-C18))[c]	5.797	5.775	5.932	6.012
d(H8−(Me-C17))[c]	5.464	5.659	5.393	5.565
d(H8−(Me-C18))[c]	6.105	5.992	6.286	6.294
d(H7−(Me-C17))[c]	3.914	3.972	3.914	3.972
d(H7−(Me-C18))[c]	5.060	4.909	5.224	5.158
	dihedrals (deg)			
	1a	**1a$^+$**	**2a**	**2a$^+$**
C2−N1−C4−C6	176.91 (4.21)[d]	170.32 (15.97)[e]	173.72	172.78
C2−N1−C4−O2	−0.78 (−174.01)[d]	−5.34 (−167.44)[e]	−3.56	−3.29
N1−C4−C6−C5	−60.82 (−119.75)[d]	−62.52 (51.13)[e]	−57.90	−58.57
N1−C4−C6−C7	127.87 (65.19)[d]	128.69 (−132.64)[e]	130.61	133.01
N1−C2−C10−C11	−50.74 (−167.50)[d]	−39.44 (−68.04)[e]		
C3−C2−C10−C11	66.34 (80.34)[d]	77.04 (178.62)[e]		
C2−C10−C11−C12	−84.92 (−100.84)[d]	−75.87 (−74.56)[e]		
C2−C10−C11−C16	96.20 (78.48)[d]	104.94 (105.03)[e]		

[a] See Tables 1−4 in the Supporting Information for the PDB-formatted coordinates. [b] Average distances to all carbon atoms of the benzene group and respective deviations are shown. [c] Me stands for methyl group. [d] X-ray data for **1a** is shown in parentheses (see ref 3a). [5] X-ray data for **1b**, which is the methylated analogue of **1a**$^+$, is shown in parentheses (see ref 3a).

of larger number of nearby methyl protons which are available for relaxation of the cis methine proton in the former.[12b]

In our studies, it has been observed (Table 1) that all pyridinyl (pyridinium) protons in the standard **2a** and **2a**$^+$ have longer T_1 than those in **1a** and **1a**$^+$, respectively, owing to the presence of the neighboring phenyl group in the later. This suggests that the pyridinyl (pyridinium) protons in **1a** or **1a**$^+$ relax through the protons of the neighboring phenyl group, and therefore showing a quicker relaxation rate than the standards **2a** and **2a**$^+$, which clearly backs up the proposed CH (pyridinyl)−π (phenyl) interaction at the neutral state, and cation (pyridinium)−π (phenyl) interaction in the protonated state. Since the spin−lattice characters of the neutral (**1a** and **2a**) and protonated (**1a**$^+$ and **2a**$^+$) species are very different because of their different hydration properties (compare the $\Delta G°_{sol}$ from ab initio calculations, Table 3), it is more correct to compare the neutral **1a** with **2a** and the protonated **1a**$^+$ with **2a**$^+$. Hence, the ΔT_1 [i.e., $(T_1)_{\mathbf{2a}} - (T_1)_{\mathbf{1a}}$] shows (row 9 in Table 1) that, for **1a**, the H5 relaxes more quickly than any other protons of the pyridinyl ring (by 9.2 s, with respect to that of the standard **2a**) followed by H9 (5.5 s) and the slowest relaxing protons being H7 (3.0 s) and H8 (3.3 s). This means that the H5 and H9 of **1a** have relaxation pathways available through the neighboring phenyl group, thereby suggesting that the H5/H9 edge of pyridinyl group is interacting preferentially with the π face of the phenyl moiety over that of the H7/H8 face. Similarly, in the protonated state, **1a**$^+$, $\Delta T_1{}^{\neq}$ [i.e., $(T_1)_{\mathbf{2a}^+} - (T_1)_{\mathbf{1a}^+}$] for H5 (4.7 s) and H9 (3.9 s) show (row 10 in Table 1) that they relax quicker compared to H7 (2.3 s) and H8 (1.7 s) because of the spatial proximity of the phenyl group to the H5/H9 edge of the pyridinium group. Thus, this T_1 relaxation study clearly supports our conclusion based on the chemical shift studies (see above) that the edge-to-face electrostatic interaction between pyridinyl/pyridinium and phenyl groups predominates in the aqueous solution over the face-to-face interaction in the solid state.

F. Molecular Modeling by ab Initio Simulations. We have built ab initio optimized models for **1a**, **1a**$^+$, **2a**, and **2a**$^+$ using the Gaussian 98 program package.[13] Gas-phase-optimized molecular geometries have been obtained at the Hartree−Fock (HF) level using 6-31G** basis set starting from HF/3-21G* optimized geometries and assuming HF energy convergence threshold equal to 10^{-7} au with simultaneous fulfillment of standard Gaussian's Maximum Force, RMS Force, and RMS Displacement criteria. The thermochemical contributions[13,16a] to the proton affinities[16] have been estimated in the HF analytical frequencies calculations. The influ-

(13) Gaussian 98 (Revision A.6): Frisch, M. J.; Trucks, G. W.; Schlegel, H. B.; Scuseria, G. E.; Robb, M. A.; Cheeseman, J. R.; Zakrzewski, V. G.; Montgomery, Jr., J. A.; Stratmann, R. E.; Burant, J. C.; Dapprich, S.; Millam, J. M.; Daniels, A. D.; Kudin, K. N.; Strain, M. C.; Farkas, O.; Tomasi, J.; Barone, V.; Cossi, M.; Cammi, R.; Mennucci, B.; Pomelli, C.; Adamo, C.; Clifford, S.; Ochterski, J.; Petersson, G.; Ayala, P. Y.; Cui, Q.; Morokuma, K.; Malick, D. K.; Rabuck, A. D.; Raghavachari, K.; Foresman, J. B.; Cioslowski, J.; Ortiz, J. V.; Baboul, A. G.; Stefanov, B. B.; Liu, G.; Liashenko, A.; Piskorz, P.; Komaromi, I.; Gomperts, R.; Martin, R. L.; Fox, D. J.; Keith, T.; Al-Laham, M. A.; Peng, C. Y.; Nanayakkara, A.; Gonzalez, C.; Challacombe, M.; Gill, P. M. W.; Johnson, B. G.; Chen, W.; Wong, M. W.; Andres, J. L.; Head-Gordon, M.; Replogle E. S.; Pople, J. A. Gaussian, Inc., Pittsburgh, PA, 1998.

(14) (a) Cances, M. T.; Mennucci V.; Tomasi, J. *J. Chem. Phys.* **1997**, *107*, 3032. (b) Barone V.; Cossi, M. *J. Phys. Chem.* **1998**, *109*, 6246.

(15) (a) Miertus, S.; Scrocco E.; Tomasi, J. *J. Chem. Phys.* **1981**, *55*, 117. (b) Miertus S.; Tomasi, *J. Chem. Phys.* **1982**, *65*, 239. (c) Cossi, M.; Barone, V.; Cammi R.; Tomasi, *J. Chem. Phys. Lett.* **1996**, *255*, 327.

(16) (a) Schüürmann, G.; Cossi, M.; Barone, V.; Tomasi, J. *J. Chem. Phys.* A **1998**, *102*, 6706. (b) Chen, I.-J.; MacKerell, A. D., Jr. *Theor. Chem. Acta* **2000**, *103*, 483. (c) Liptak, M. D.; Shields, G. C. *J. Am. Chem. Soc.* **2001**, *123*, 7314.

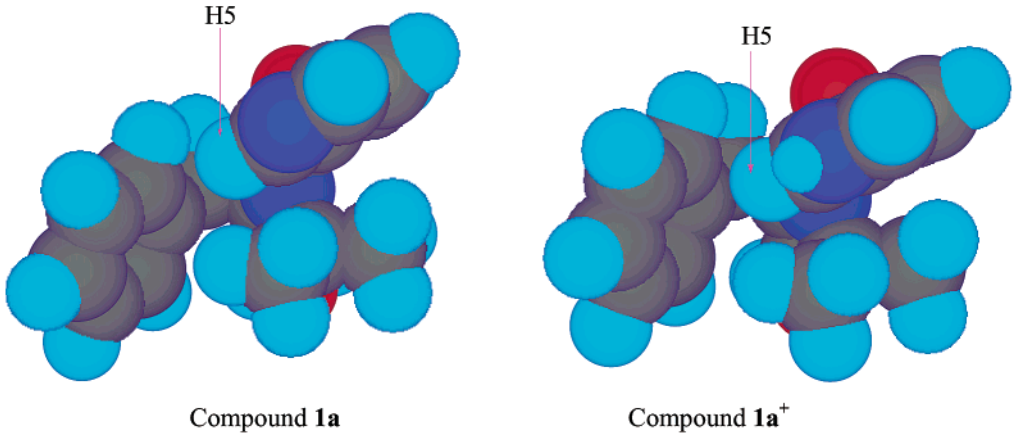

FIGURE 3. Gas-phase ab initio optimized geometries of compounds **1a** and **1a**$^+$. It is noteworthy that the H5 of pyridinyl (see Scheme 1 for numbering) is more on the periphery of the face of the phenyl ring in **1a**, whereas in **1a**$^+$, the H5 of pyridinium is facing right at the central part of the phenyl ring in the edge-to-face interactions.

ence of the water−solvent media has been examined within the polarized continuum model (PCM)[15] utilizing the polarized conductor calculation model (COSMO),[14b] integral equation formalism (IEFPCM),[14a] and the original PCM reaction field using the polarizable dielectric model.[15] Our observations are as follows:

(1) The comparison of $\Delta\Delta G° = (\Delta G°_{\mathbf{1a}^+} - \Delta G°_{\mathbf{1a}})$ and $\Delta\Delta G° = (\Delta G°_{\mathbf{2a}^+} - \Delta G°_{\mathbf{2a}})$ show that the protonation of **1a** to **1a**$^+$ stabilizes the pyridinium−phenyl−methyl system by 2.38 kcal mol^{-1} compared to the protonation of **2a** to **2a**$^+$. Whereas a thermochemical estimation of the $\Delta G°_g$ from the frequency calculations shows no significant difference in the process of protonation of **1a** and **2a** (Table 3).

(2) The solvation study at the gas-phase geometry showed that the protonation of **2a** to **2a**$^+$ has more stabilizing effect compared to protonation of **1a** to **1a**$^+$ (Table 3). This presumably reflects the relative hydrophobicity of **1a** /**1a**$^+$ compared to **2a** /**2a**$^+$ owing to the phenyl group in the former pair.

(3) The gas-phase geometries of **1a** and **1a**$^+$ are shown in Figure 3, whereas essential geometrical parameters are shown in Table 4. Actual coordinates of **1a** and **1a**$^+$ are shown in PDB format in the Supporting Information. It can be seen from the stereochemical orientation of the pyridine/pyridinium group that the H5 edge is almost perpendicularly oriented to the face of the phenyl group owing to the edge-to-face interaction, as experimentally found by us by the pH-dependent proton chemical shift titration method. The distance between phenyl- and H5 proton of pyridine/pyridinium groups of **1a** and **1a**$^+$ decreases by 0.7 Å (Table 4) upon protonation, thereby substantiating our observation that an electrostatic pyridinium (cation)−phenyl (π) interaction is relatively stronger than the neutral pyridinyl-phenyl interaction.

Conclusions

(1) Our present study has given a straightforward experimental evidence of the intramolecular aromatic interaction between pyridinium and neighboring phenyl groups through the stabilization of weak cation−π interaction[4] in protonated nicotinamide derivatives **1a**$^+$, thereby making the pyridine−nitrogen more basic (pK_a 2.92) compared to that in the standard **2a**$^+$ (pK_a 2.56). This pK_a differences (Table 1) show that the free energy of the cationπ interaction ($\Delta\Delta G^o_{\mathrm{pKa}}$[10c] $\approx \Delta G^o_{\mathrm{cation}-\pi}$) between pyridinium and phenyl moieties is −2.1 kJ mol^{-1}. It has also been found that both the protons of pyridinium moiety of **1a** and those of the phenyl group (except δH13/H15, vide infra) showed the pK_a for the protonation of pyridinyl-nitrogen, thereby providing a direct evidence of a cross-talk in the coupled system **1a**$^+$.

(2) The relative upfield shifts (see Table 2 and Figure S4 in the Supporting Information) for the aromatic protons of pyridinium moiety in **1a**, **1a**$^+$, **1b**, **2a**, **2a**$^+$, and **2b** show that the electronic environments around the marker protons in the methylated compound (**1b** and **2b**)-are the same as those of the protonated derivative (**1a**$^+$ and **2a**$^+$), which shows that **1a**$^+$ is a good model for **1b**.

(3) It has been shown that the H5/H9-edge of pyridinium group in **1a**$^+$ is more affected than the H7/H8-edge due to the electrostatic interaction with phenyl (π) ring. This constitutes a direct evidence for an edge-to-face aromatic interaction in aqueous solution rather than the face-to-face stacking in **1a**$^+$ found in the solid state. Most important observation is the fact that this edge-to-face interaction in solution is capable of influencing the pK_a of pyridinium in **1a**$^+$ by charge donation through cation-π interaction.

(4) The absence of the charge-transfer band in UV indicates[3a] that the attractive Coulombic interaction is the dominant component in the electrostatic mediated charge transfer through the electron-deficient pyridinium to the electron-rich phenyl moieties in **1a**$^+$.

(5) The protonation of pyridine moiety (i.e., formation of pyridinium cation) promotes the electrostatics mediated partial charge donation[6a] from neighboring phenyl (π) moiety to the pyridinium due to cation-π interaction in **1a**$^+$, thereby causing the charge depletion at the phenyl moiety, which in tandem reduces the strength of the methyl CH-π interaction between phenyl and methyl groups. The difference between pK_a values observed from the titration profile of methyl protons (pK_a 3.09) and phenyl protons (pK_a 2.91) show that the free energy of the CH (methyl)-π (phenyl) interaction ($\Delta\Delta G^o_{\mathrm{pKa}}$[10b,c] $\approx \Delta G^o_{\mathrm{CH}-\pi}$) is −0.8 kJ mol^{-1}, whereas the $\Delta G^o_{\mathrm{cation}-\pi}$ of −2.1

kJ mol^{-1} has been found for the stablization of the pyridinium cation-π (phenyl) interaction.

(6) Since the pK_a is a measure of the ground-state stability of the anionic or the cation form of the product, we can estimate the electrostatic free-energy of strabilization[10] at the pK_a by the term, ΔG^o_{pKa}, which can be obtained from the following equation:[10] $\Delta G^o_{pKa} = 2.303RTpK_a$. Because we observe the pK_a of the pyridine moiety of **1a** through the pH-dependent downfield shifts of both phenyl and methyl protons, it suggests that the net electrostatic mediated charge transfer[6a,b] from the phenyl to the pyridinium through cation (pyridinium)$-\pi$ (phenyl) interaction and its effect on the CH (methyl)$-\pi$ (phenyl) interaction corresponds to ΔG^o_{pKa}[10c] of the pyridinium ion, which is ca. 17.5 kJ mol^{-1}. Most importantly, this means that the aromatic characters of the phenyl and the pyridinium rings in **1a**$^+$ are electronically coupled, and have been cross-modulated in tandem proportional to ΔG^o_{pKa} of ca. 17.5 kJ mol^{-1}. Thus the cross-modulation of electronically coupled pyridine$-$phenyl$-$methyl system is driven by the electrostatics as the engine, and the origin of this electrostatics is a far away point in the molecule$-$the pyridinyl-nitrogen.

(7) We have thus demonstrated above that a simple 1D NMR based pH-dependent titration profile can be used as a major experimental tool to identify nature of aromatic interaction provided the complex has a protonation or a deprotonation site. Interestingly, such titration method also gives an enormous insight into the energetics, geometry as well as the nature of weak noncovalent contribution in such aromatic interactions, which are of great importance in molecular recognition pattern in both biological as well as nonbiological system.

Experimental Section

(A) pH-Dependent ^{1}H NMR Measurement. All NMR experiments for compounds **1a**, **1b**, **2a**, and **2b** (Scheme 1) were performed on Bruker DRX-500 spectrometers. The NMR sample for compounds all compounds were prepared in D_2O solution (concentration of 2 mM in order to rule out any chemical shift change owing to self-association[3a]) with $\delta_{DSS} = 0.015$ ppm as internal standard (with respect to $\delta_{TMS} = 0.00$ ppm).[11] All pH-dependent NMR measurements have been performed at 298 K. The pH values (with correction of deuterium effect) correspond to the reading on a pH meter equipped with a calomel microelectrode (in order to measure the pH inside the NMR tube) calibrated with standard buffer solutions (in H_2O) of pH 4 and 7. The pD of the sample has been adjusted by simple addition of micro liter volumes of D_2SO_4 solutions (0.5, 0.1, and 0.01 M). The assignments for all compounds have been performed on the basis of selective homonuclear (^{1}H) decoupling experiments (see ref 3 and the Supporting Information for details). All spectra have been recorded using 32 K data points and 64 scans for ^{1}H.

All T_1 experiments at both neutral and protonated states for **1a** and **2a** were carried out using inversion$-$recovery technique at 298 K. Pulse lengths of 90° and 180° were calibrated prior to each experiments. Twelve relaxation delays were utilized in each experiments for determination of T_1. The fit of area and intensity of a particular signal were averaged to obtain the T_1 using Bruker software.

(B) pK_a Determination, The pH-dependent (over the range of pH 1.05$-$6.7, with an interval of pH 0.1$-$0.25, each pH has been measured two time before and after the NMR measurement and the average was taken) ^{1}H chemical shift (δ, with error $\pm$ 0.001 ppm) shows a sigmoidal titration curves. Chemical shift variations at average 35 (for **1a**) or 30 (for **2a**) different pH values have been measured to obtain the sigmoidal curves (panels A$-$H for **1a** and panels I$-$L for **2a** in Figure 1). The pK_a determination is based on the Hill plot analysis using the equation pH = log((1 $-$ α)/α) + pK_a, where α represents fraction of the protonated species. The value of α is calculated from the change of chemical shift relative to the protonated (P) state at a given pH ($\Delta_P = \delta_N - \delta_{obs}$ for protonation, where δ_{obs} is the experimental chemical shift at a particular pH), divided by the total change in chemical shift between neutral and protonated (P) state (Δ_{N-P}), which is shown for each titration plot in Figure 1. So the Henderson$-$Hasselbalch-type equation[10a] can then be written as pH = log(($\Delta_{N-P} - \Delta_P$)/Δ_P) + pK_a. The pK_a is calculated from the linear regression analysis of the Hill plot (panels a$-$h for **1a** and Panels **i**$-$**l** for **2a** in Figure 2).

Acknowledgment. Generous financial support from the Swedish Natural Science Research Council (Vetenskapsrådet), the Stiftelsen för Strategisk Forskning, Philip Morris Inc (to J.C.) and Grant-in-Aid for Scientific Research (C) (no. 13650901) from the Japan Society for the Promotion of Science (to S.Y.) is gratefully acknowledged.

Supporting Information Available: Figure S1A$-$S1B: ^{1}H NMR plots of aromatic protons and methyl chemical shifts as a function of pH for compounds **1a** at 298 K (only 13 representative pH-dependent chemical shifts including the lowest and highest pHs are shown out of total 35). Figure S2: ^{1}H NMR plots of aromatic protons chemical shifts as a function of pH for compounds **2a** at 298 K (only 13 representative pH-dependent chemical shifts including the lowest and highest pHs are shown out of total 35). Figure S3A$-$S3B: ^{1}H NMR spectra for **1a**, **1b**, **2a**, and **2b** in D_2O at 298 K. Figure S4: NMR plots of selective homonuclear (^{1}H) decoupling experiments in D_2O at 298 K for **1a** for assignments. Tables 1$-$4 show for the coordinates of free-optimized ab initio geometries of compounds **1a**, **1a**$^+$, **2a**, and **2a**$^+$ in PDB format. This material is available free of charge via the Internet at http://pubs.acs.org.

JO026572E